Mansoura Engineering Journal

Volume 47 | Issue 1 Article 11

5-14-2022

Shoreline Changes Detection Using Digital Shoreline Analysis System: Case Study Damietta – Port Said Coastal Area, Egypt.

Ahmed Tharwat Sarhan
Master of Science Student, coastal and Marine Engineering, ahmedtharwat187@std.mans.edu.eg

Moheb Mina Iskander
Professor of Coastal Engineering, Head of the Hydrodynamic Department, Coastal Research Institute, National Water Research Center, Egypt., moheb_iskander@nwrc.gov.eg

Karim Nassar
Assistant Professor in Irrigation Engineering and Hydraulics Department, School of Civil Engineering, Faculty of Engineering, Mansoura University, karim.nassar@ejust.edu.eg

Mahmoud El-Gamal
Professor of water structure, Mansoura university, Mansoura, Egypt., mmelgamel@hotmail.com

Recommended Citation

Tharwat Sarhan, Ahmed; Mina Iskander, Moheb; Nassar, Karim; and El-Gamal, Mahmoud (2022) "Shoreline Changes Detection Using Digital Shoreline Analysis System: Case Study Damietta – Port Said Coastal Area, Egypt.," *Mansoura Engineering Journal*: Vol. 47 : Iss. 1 , Article 11.
Available at: https://doi.org/10.21608/bfemu.2022.236869

Mansoura University
Faculty of Engineering
Mansoura Engineering Journal

Shoreline Changes Detection Using Digital Shoreline Analysis System: Case Study Damietta – Port Said Coastal Area, Egypt

Ahmed Tharwat Sarhan*, Moheb Mina Iskander, Karim Nassar and Mahmoud El Gamal

KEYWORDS:
Damietta shoreline, Port Said shoreline, Shoreline change, DSAS, Landsat images.

***Abstract*— The Nile Delta of Egypt suffers from many coastal problems due to natural and human factors specially the eastern part from Damietta to Port Said. The aim of this paper is to investigate the coastal problems within the eastern part of the Nile Delta. This investigation depends on monitoring the frequency of change of the shoreline along Damietta Port Said shoreline. The Digital Shoreline Analysis System (DSAS) which is an extension for ARCGIS 10.5 was used to analyze shoreline change rates by using satellite images. Six Landsat multi-temporal satellite images of years (2002, 2004, 2006, 2010, 2015 and 2020) were used to detect shoreline erosion and accretion patterns for the study area. These images were geometrically and radio-metrically rectified to be used in the analysis of shoreline change rates. DSAS tool with its three methods: End Point Rate (EPR), Linear Regression Rate (LRR), and Net Shoreline Movement (NSM) were used to identify the shoreline change rates. The results showed that the study area has faced many shoreline changes that differ between accretion and erosion. It is clear that coastal structures, human activities and the hydrodynamic forces are the main reasons of the shoreline changes within the study area.**

I. INTRODUCTION

THE coastal zone can be considered as one of the most active, complicated, and sensitive geomorphic units which need to be monitored continuously to track the changes in shorelines [1]. Before constructing the high Aswan dam, the discharge of sediment from the Damietta branch of the Nile was estimated to be about 0.6 to 1.8 million m^3/year which was the main reason for shoreline progression to the seaside. After constructing the high Aswan dam the sediment discharge to the sea became negligible which led to progress erosion and accretion within the coastal area due to the human impacts. These changes caused a lot of losses in infrastructures and investments near the coastline [2]. The studies admitted that shoreline monitoring, extraction, and calculation of change rates are indispensable. The aim of this study is to identify the erosion accretion rates, source of the sediment and the expected shoreline changes along the area from Damietta to Port Said, Northeastern coast of Egypt. Dewedar and Frihy [3] calculated the annual rate of shoreline change using digital shoreline analysis software (DSAS) along the north-western coast of the Nile Delta to detect the beach response to the construction of the coastal measures. Banna and Hereher [4]detected temporal coastline changes by analyzing satellite Landsat images for the Northern Sinai Mediterranean coast during the period from 1986 to 2001 to associate sediment transport. Nassar et al. [5] used DSAS to detect the change on the shoreline along the north Sinai coast of Egypt and

Received: (14 November, 2021) - Revised: (01 January, 2022) - Accepted: (19 January, 2022)

***Corresponding Author:** Ahmed Tharwat Sarhan, Master of Science Student, coastal and marine engineering. (Email: ahmedtharwat187@std.mans.edu.eg)*

Prof. Moheb Mina Iskander, Professor of Coastal Engineering, Head of the Hydrodynamic Department, Coastal Research Institute, National Water Research Center, Egypt. (E-mail: moheb_iskander@nwrc.gov.eg)

Dr. Karim Nassar, Assistant Professor in Irrigation Engineering and Hydraulics Department, School of Civil Engineering, Faculty of Engineering, Mansoura University. (E-mail: Karim.nassar@ejust.edu.eg)

Prof. Mahmoud El-Gamal, Professor of water structure, Mansoura university, Mansoura, Egypt. (E-mail: Mmelgamel@hotmail.com)

(Ser. NO. BFEMU-2111-1189)

quantify erosion and accretion of the shoreline. Islam et al. [6] studied the shoreline changes along a 65 km shoreline of the Kutubdia island, southeast Bangladesh using DSAS tool for the period between 1974 and 2014. Sarhan et al.[7] monitored the shoreline changes of El Hammra port northwest Egypt using histogram threshold of band 5.

II. STUDY AREA

Damietta promontory is considered one of the most important industrial area along the Nile Delta coast that extends about 240 km from Alexandria to Port Said [8]. The coastline of the zone of concern extends about 40 km along the northeastern Nile Delta coast of Egypt between Damietta and Port Said. The study area located between latitudes (31°25'40"N to 31°16'23.85"N) and longitudes (31° 59' 52" E to 32°19'4.92"E) as shown in Figure 1. Measurements of the directional wave for the study region in 2010 showed that the maximum recorded wave height during storms is nearly 6.0 m from NW direction, while the maximum wave height is 4.2 m from N direction. The maximum peak wave period ranges between 7.0 and 13.2 s. Khalifa et al. [9] mentioned that the predominant wave direction throughout is from the N-NW (86%) sector for all months (mainly from NNW (49%) direction). The movement of the littoral current is normally eastwards with an average velocity of about 34 cm / s. The Damietta promontory is a semi-diurnal micro-tidal inlet with a tidal range of 25-30 cm [9].The beach of the area consists of loose quartz sand merged with little amounts of heavy minerals and shell fragments. The study area was divided into five zones.

Figure 2 demonstrates the five zones, each part of the first four zones extends for 7350 m and divided into 147 transects. The first zone is from transects 1 to 147. It extends from latitudes (31°25'40"N to 31°22'00"N) and longitudes (31° 59' 52" E to 32°3'00"E). The second zone extends from transect 148 to 294. It extends from latitudes (31°19'30"N to 31°23'00"N) and longitudes (32° 2' 00" E to 32°6'30"E). The third zone extends from transect 295 to 441 within latitude (31°18'00"N to 31°21'30"N) and longitudes (32° 6' 30" E to 32°10'30"E). The fourth zone extends from transect 442 to 588 with latitude (31°16'00"N to 31°19'30"N) and longitudes (32° 10' 30" E to 32°14'00"E). The fifth zone extends from transect 589 to 738 with latitude (31°15'30"N to 31°19'00"N) and longitudes (32° 14' 00" E to 32°18'30"E).

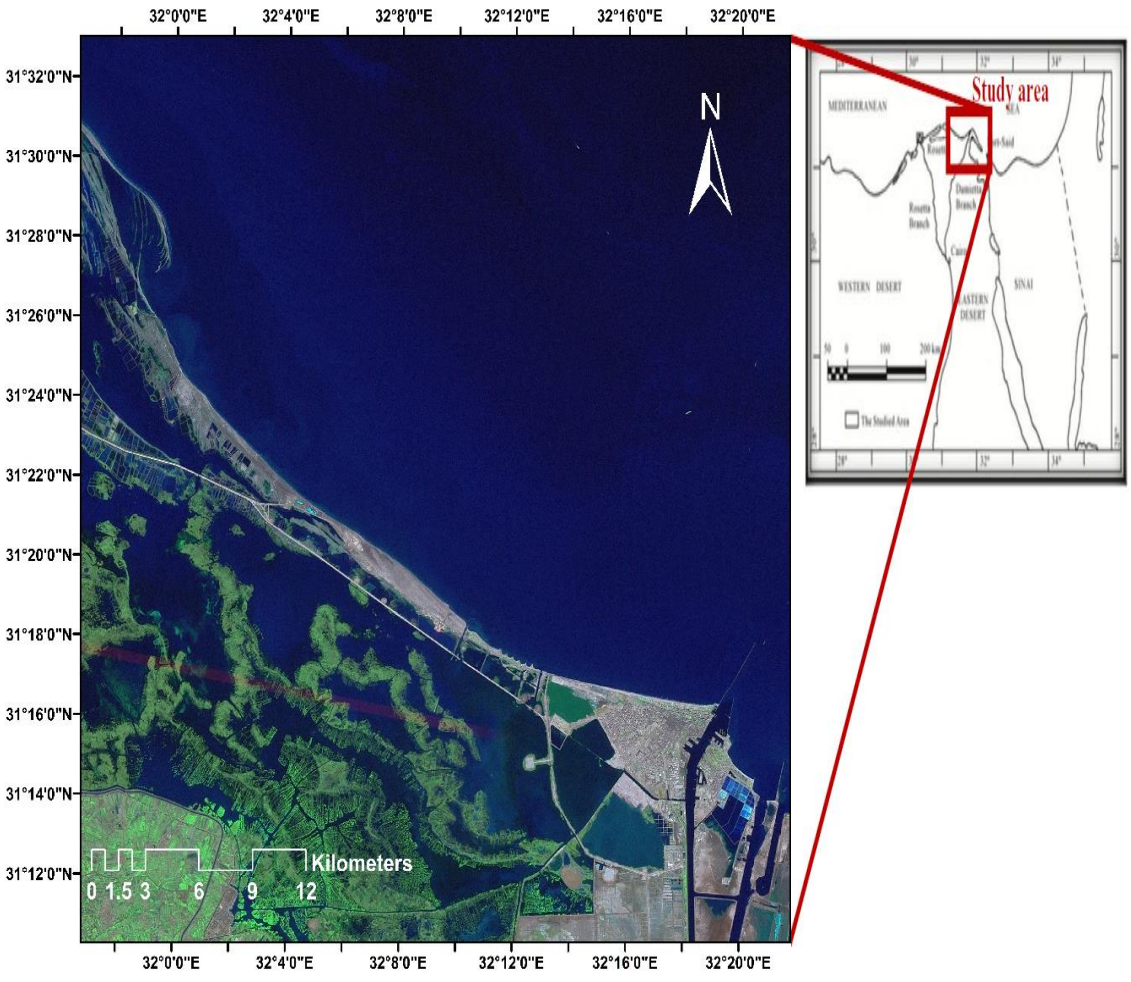

Fig. 1. The study area extends 40 km from Damietta to Port Said , 2002 satellite image

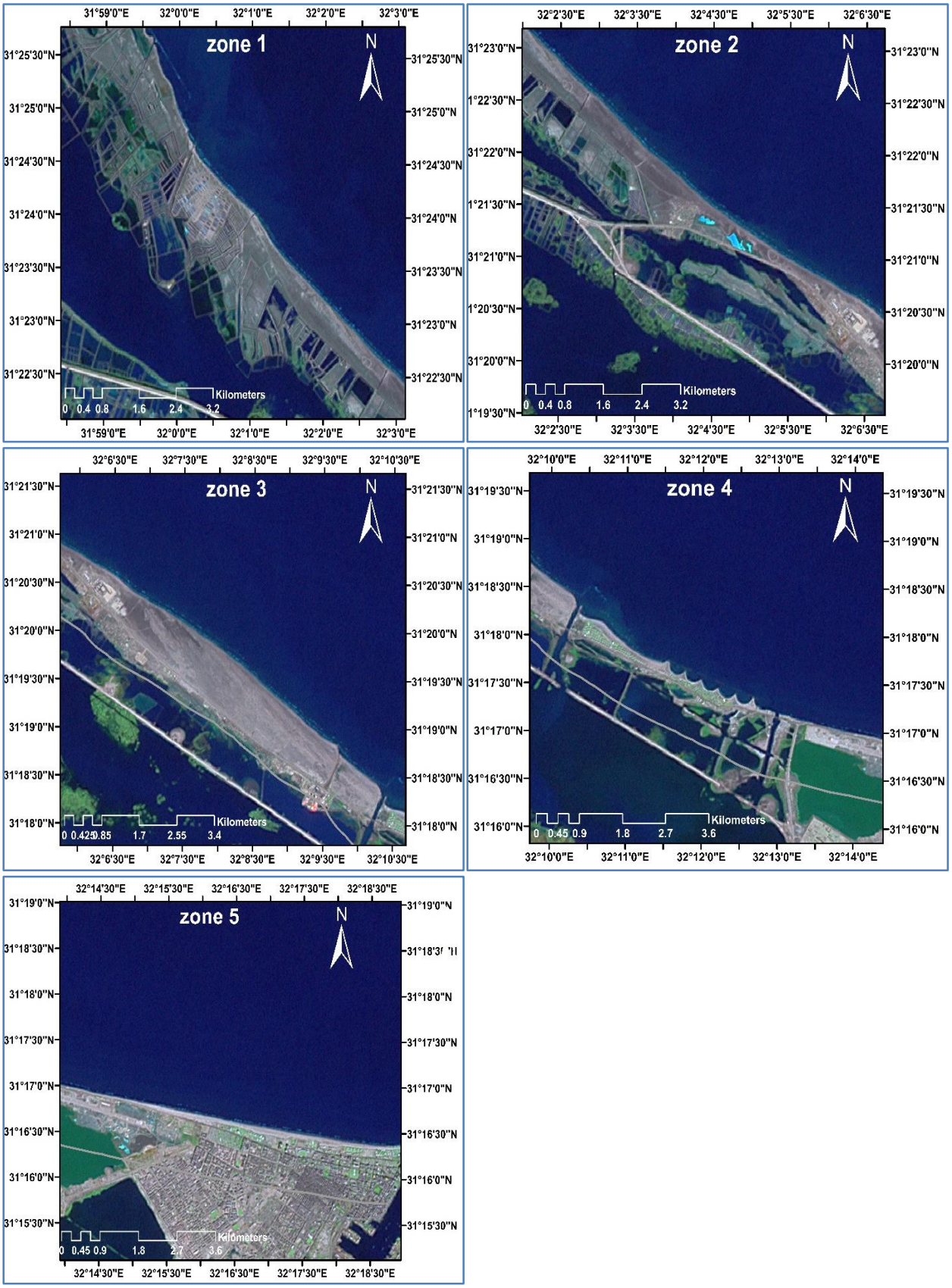

Fig. 2. The five zones of the study area which used in this study, satallite image of 2002.

III. MATERIAL AND METHODS

A. *Data Sources:*

The shorelines used in this study were extracted from six satellite images from 2002 to 2020 (2002, 2004, 2006, 2010, 2015, 2020).

Five satellite images were acquired from the U.S Geological Survey (USGS) earth explorer website. Landsat 5 (Thematic mapper) images are used for the period from 2002 to 2010 then the rest period to 2020 are collected from Landsat 8 (OLI/TIRS) to cover 18 years from 2002 to 2020.

Table 1 presents the acquired images from U.S geological website https://earthexplorer.usgs.gov/

TABLE I
DETAILS OF SATELLITE IMAGES ACQUIRED IN DIFFERENT YEARS VIA https://earthexplorer.usgs.gov/

Year of acquisition	Satellite data	Sensor	Path /Row	Resolution
2002	Landsat 5	TM	176/38	30
2004	Landsat 5	TM	176/38	30
2006	Landsat 5	TM	176/38	30
2010	Landsat 5	TM	176/38	30
2015	Landsat 8	OLI/TIRS	176/38	30
2020	Landsat 8	OLI/TIRS	176/38	30

B. Satellite Images Processing:

The main satellite images processing operations are geometric rectification and radiometric correction. Firstly, the geometric correction operation was carried out using 30 ground control points like streets intersection. This operation was carried out using ENVI 4.8 software so that we can eliminate the distortions due to tilt, scale variation, and lens distortions. The second step is radiometric correction which is done in a single step using ENVI 5.3 software, that combines sensor calibration with the atmospheric correction and the view angle and sun effects. The required parameters (offset/gain, sun elevation, and satellite viewing angles) collected from the Landsat metadata documentation. Finally, all rectified images are exported to ArcGIS 10.5 software to digitize the coastal shoreline.

C. Shoreline Extraction Procedure:

The shoreline is mainly defined as the separating line between land and sea. The wet/dry line is the most widely used proxy to detect the shoreline location and is a valid coastal change predictor for many coastal areas [10]. There are several steps to extract the shoreline by using DSAS software that can be summarized as following, the initial step is detecting method to extract shoreline in this study is band 5 histogram threshold method that use band 5 for each Landsat image from different years. Band 5 has wavelength of water reflectance approximately equals zero. The first step is the extraction of binary image by raster calculator which consider water pixels equal zero and the land pixels values equal 1. The second step is converting raster to polygon, then converting polygon to line. The most important thing is trying to get the shoreline as a single polyline in one length. The most important step is the projection of the extracted shoreline to the universal transverse Mercator with reference to UTM zone 36 N datum. Figure 3 shows the Flow chart of the methodology to identify the shoreline change rates.

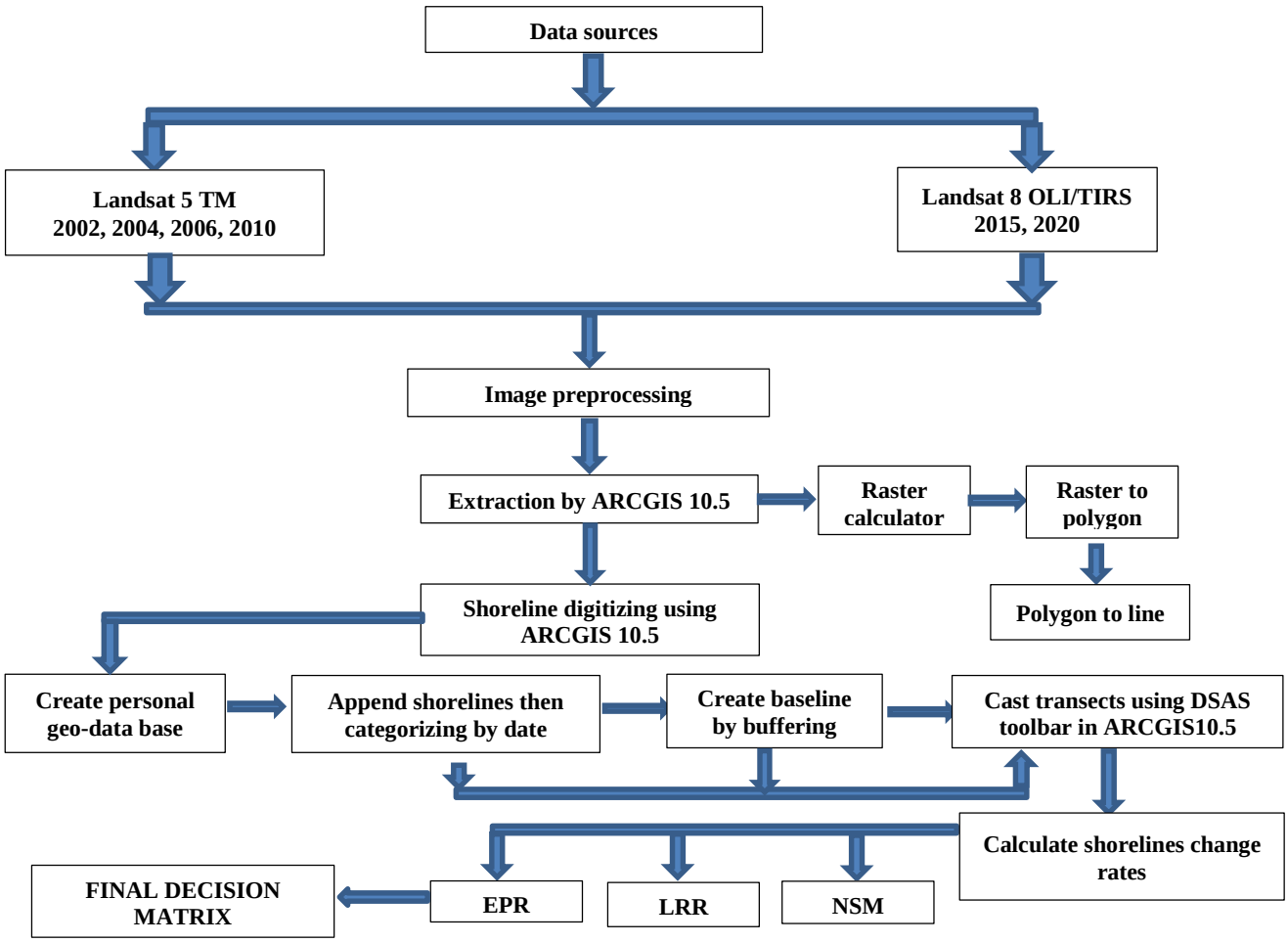

Fig. 3. Flow chart of the methodology to identify the shoreline change rates

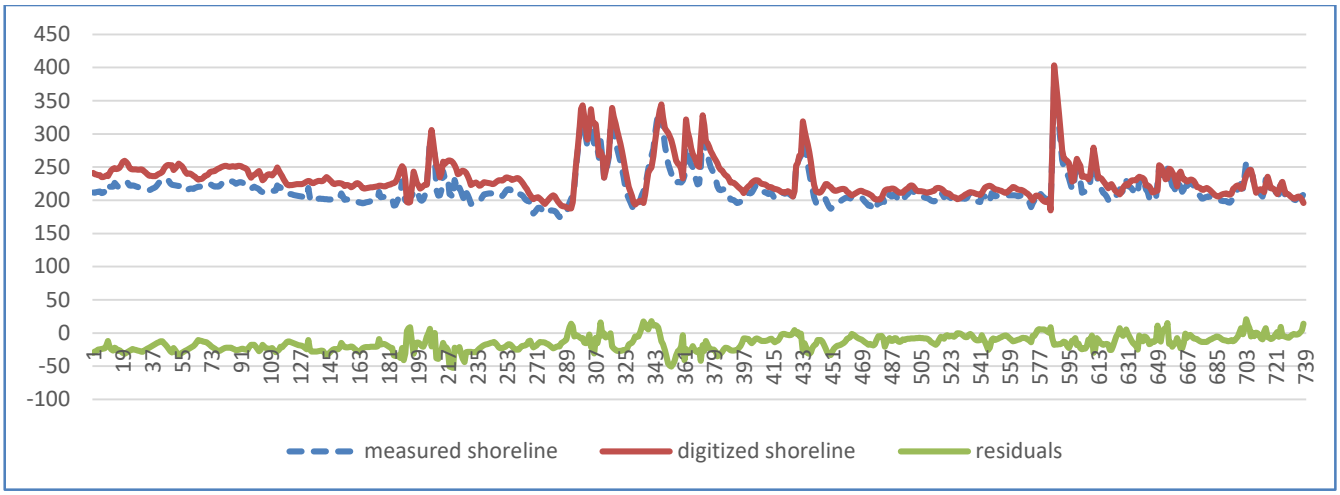

Fig. 4. Difference between digitized shoreline from image and the measured shoreline from field as well as the residuals between them for the year 2020.

D. Validation Procedure:

Validation process is executed using DSAS tool. Field measurement of the shoreline along the study area was surveyed in 2020 using DGPS and compared with the extracted from the satellite images within the same period. The comparison is identified along the 739 transects to calculate the difference between the two shorelines in each transect. The **Normal Root Mean Square for the Error (NRMSE)** equals 0.0893 only along the study area. Figure 4 presents the measured shoreline from the field, the digitized one from the satellite image and the residuals between them.

E. Shorelines Change Rates Calculation Methods:

Shoreline change rates and distance between shorelines were calculated in this study by using three methods of the DSAS tools, which are (EPR, LRR, and NSM). The **EPR** stands for Endpoint Rate which equals the distance between the two shorelines divided by the number of years between them.

The second method to calculate shoreline movement is the Linear Regression Rate (**LRR**), which can be determined by fitting least-squares regression line to all points of shorelines for a particular transect. This method has some features such as all the points of shorelines data are used regardless of the change of trend in the change rate or accuracy, purely computational, and easy to be used. The third method is Net Shoreline Movement (**NSM**), it is a distance, not a rate that describes the total distance between the two shorelines the old one and new one. The negative value of these three methods indicates landward movement of the shoreline which is called erosion process, while the positive sign indicates seaward movement of the shoreline which is called accretion process. Natesan et al. [11] classified the rate of change of shorelines into seven categories depends on LRR values as shown in the following Table 2:

TABLE II
CLASSIFICATION OF LBR EROSION AND ACCRETION RATES ACCORDING TO NATESAN, et al., 2015 CLASSIFICATION.

Category	Rate of shoreline change (m/year)	Shoreline rate classification
1	> -2	Very high erosion
2	> -1 but < -2	high erosion
3	> 0 but < -1	moderate erosion
4	0	Stable
5	> 0 but < +1	Moderate accretion
6	> +1 but < +2	High accretion
7	> +2	Very high accretion

IV. RESULTS AND DISCUSSIONS

A. Shoreline Change Rate Analysis

The shoreline was extracted from the images of 2002, 2004, 2006, 2010, 2015, and 2020 as shown in Figure **5**. The analysis of shoreline change rates was conducted using DSAS tool, which is an ARCGIS 10.5 extension. This procedure started with creation of personal geo-database in ARCGIS 10.5 for the extracted shorelines. it has an attribute table as well as some attributes to be defined are ID, DATE, Shape length, and uncertainty. The date of satellite image is filled in the date column and the other data are automatically generated. The Uncertainty column is filled depends on the year of picture acquisition and its resolution. After that, the six shorelines are appended in one shape file. A baseline was buffered parallel to the shoreline of 2020 with offset of 1200 m. The transects are casted perpendicular to the baseline with spacing 50m. Then the rates of erosion and accretion are calculated by several statically models which is the output part from DSAS tool. Zone 4 results were taken as an example for the rest of the five zones. Figure **6** and Figure **8** show EPR rates through the five successive periods in zone 4. For the first period from 2002 to 2004 it is clear that, the maximum EPR accretion rate is +83.62 m/year at transect no. 450 then it decreases gradually eastward to reach nearly zero in some transects greater than no. 530. The mean accretion rate is 25.67 m/year. The EPR maximum erosion rate is -23.59

m/year with mean value of -6.39 m/year. For the second period from 2004 to 2006 the results show that, the maximum accretion rate is 60.78 m/year with mean value of 15.16 m/year. The maximum and mean erosion rates are -29.42 m/year and -9.05 m/year, respectively. For the third period from 2006 to 2010, the maximum accretion rate is + 43.63 m/year while the maximum erosion rate is -13.49 m/year. The mean accretion and erosion rates are +9.60 m/year and -2.25 m/year respectively. For the fourth period from 2010 to 2015, the maximum erosion rate is -16.23 m/year and the maximum accretion rate is + 14.25 m/year. The mean value of accretion and erosion rates are 4.47 m/year and -6.00 m/year, respectively.

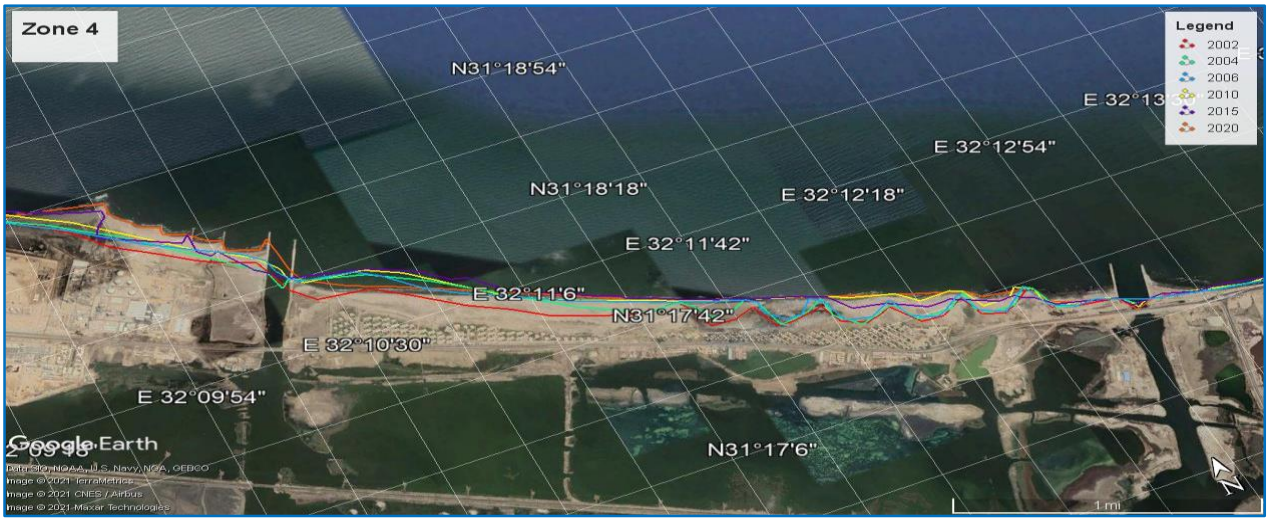

Fig.5. Shoreline changes from satellite images at Zone 4 during the period from 2002 to 2020.

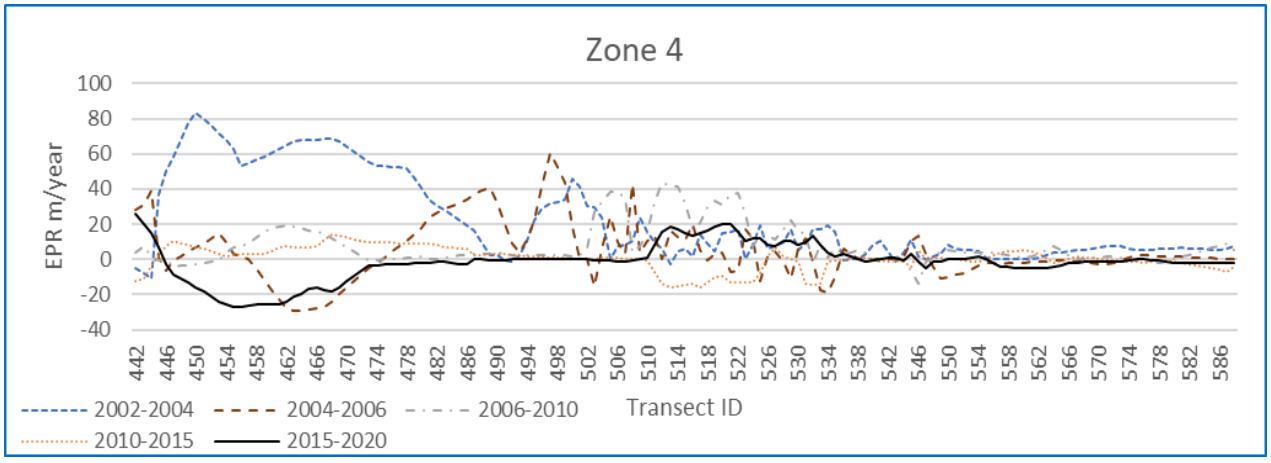

Fig.6. Shoreline change rate (End Point Rate) at Zone 4 during the period from 2002 to 2020

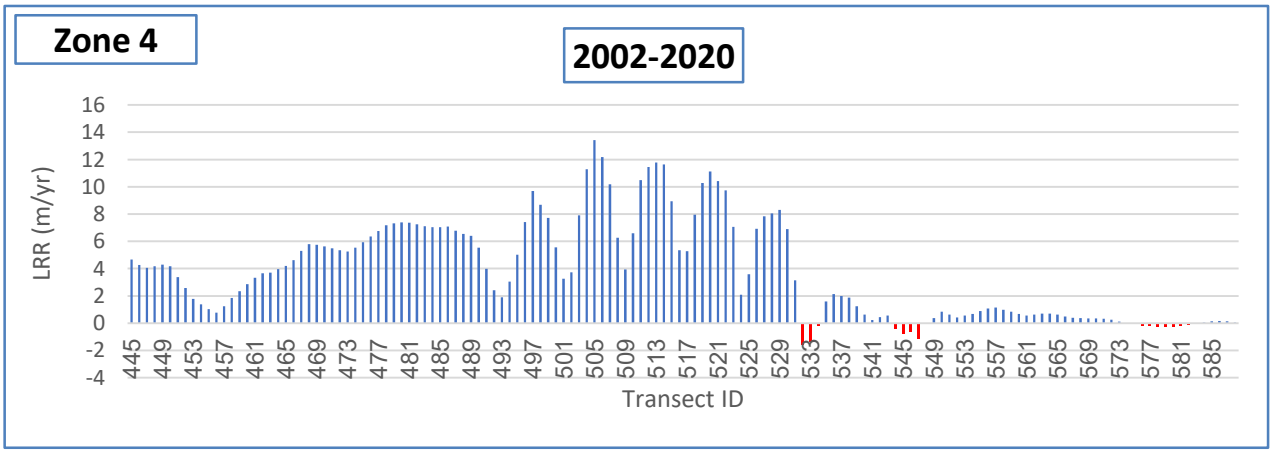

Fig.7. Linear Regression Rate (LRR) at Zone 4 during the period from 2002 to 2020

For the fifth and final period of time from 2015 to 2020, the maximum erosion rate is -27.60 m/year and the maximum accretion rate is + 25.74 m/year. The mean value of accretion and erosion rates are 7.57 m/year and -6.59 m/year respectively. Table 3 summarize the NSM and EPR maximum and mean accretion and erosion values. From Figure 7 which presents LRR rates pattern for zone 4, we can conclude that 87 % of the transects are accretion and the rest are fluctuating between minor accretion to minor erosion.

The first zone extends from transect 1 to transect 147. From 2002 to 2020, the study area fluctuates between erosion and accretion. The dominating phenomena is erosion. The percentages of erosion transect are 70.07 %, 89.12 %, 66.67%, 98.64% and 87.07% for the five successive periods respectively. The maximum EPR erosion rates are -20.34, -34.15, -20.17, -21.38 and -12.60 m/year at transects 76, 76, 5, 11, 112 for the successive periods respectively. For The second zone, from 2002 to 2004 the dominating phenomena is accretion. The accretion transects have percentage 79.59 % of the total transects. The maximum EPR accretion rate is + 18.03 m/year at transects 222, 223 ,224. After that, from 2004 to 2020 the accretion transects began to decrease in value and number. The dominating phenomena turned to be erosion through the four periods. The erosion transects have percentage of 86.39 %, 65.99 %, 61.90 %, 97.28 % for the successive four periods respectively. The maximum EPR erosion rates are - 41.0, - 21.93, -21.45, -22.90 for the successive four periods respectively. The third zone extends from transect 295 to 441. From transect 295 to 368, the dominating shoreline change process was erosion with negligible number and value of accretion transects. The erosion transects percentages are 41.50 %, 74.15 %, 60.54 %, 69.39%, 53.06 % for the successive periods respectively for the whole zone. The maximum EPR regression rates are -23.95, -18.97, -8.38, -16.22, -22.88 m/year at transects 440, 303, 311, 440, 404 for the five successive periods respectively. From transect 368 to 441, the dominating process is shoreline accretion. Maximum accretion rates have high values through these transects equal to + 45.93, +42.01, +16.67, +24.43 and + 36.07 m/year through five periods respectively. The fourth zone extends from transect 442 to 588. From 2002 to 2015, shoreline advance is the dominating process. The percentages of EPR accretion transects are 93.20 %, 61.90 %, 82.99 % and 63.27% for the four successive periods respectively. The maximum EPR accretion rates are + 83.62, + 60.87, + 43.63 and + 14.25 m/year at transects 450, 497, 512, and 468 for the successive periods respectively. We can notice that the maximum accretion zone moved through the zone then turned back to the start of the zone. This indicates the fluctuation between erosion and accretion. From 2015 to 2020, most of transects have low values of erosion and accretion except for two parts. The first part from transects 446 to 471 has the maximum EPR erosion/accretion rates equal to -27.36 and + 25.74 m/year. the second part from transects 510 to 538 has high value of accretion equals to + 20.0 m/year at transect 520. The fifth zone extends from 589 to 738. From 2002 to 2015, accretion is dominating the shoreline change process along the fifth zone. It has percentages equal to 100 %, 67.35 %, 59.18 % and 90.48 % for the successive four periods respectively. The maximum EPR accretion rates are + 17.60, + 14.28, + 15.04, + 13.02 at transects 665, 737, 681 and 695. From 2015 to 2020, the dominating process changed from accretion to be erosion. This is evident from that the sedimentation transects percentage decreased to reach 10.20 % and regression transects percentage increased to reach 89.80 %. The maximum EPR erosion rate is -10.43 m/year. This indicates that the nature of the change in the zone has varied from erosion to sedimentation. The existence of all these coastal structures along the shoreline from Damietta to Port Said has trapped huge amount of longshore sediment which led to erosion at the last period.

B. Decision Matrices Using LRR Rates Pattern:

LRR rates were calculated for all transects from all shorelines of the study area from 2002 to 2020 and presented in figure 9. We can notice that erosion is the dominating process that happens in zone one. Zone one is divided into three subzones (A, B, and C) depending on the variation in rates of erosion as shown in the LRR data curve. LRR mean values in the three zones are -6.52, -3.93, and -5.96 m/year, respectively. The main reason for these very high rates of erosion in zone 1 is the sand spit that locates west of zone 1 that trapped the longshore sediment transport within the spit west of the study area and prevent the main source of sediment that replaced the moved sediment from the study area. Another reason for these high rates is the change in the nature of the shoreline by the human intervention and the establishment of many jetties to protect the water intake of fish farms which obstacle the eastward sediment transport. Zone two can be divided into four subzones (A, B, C, and D) depending on the rates of erosion and accretion. The main issue is at zone A, where the maximum LRR mean erosion rate equals -18.27 m/year. The erosion rates decreased gradually through zone B to reach zero with LRR mean of -8.37 m/year. In zone C, the rates turned into high accretion rates with a mean value equal 1.52 m/year. In the last Zone D, the erosion rates are very high erosion with a mean value of -3.20 m/year. Subzone A is downstream the last jetty of the fish farms intakes jetties. This led to the regression of the shoreline for 270 meters alongshore. Zone three is divided into three subzones A, B and C, respectively. The erosion area located at subzone A has LRR mean rate equals -5.88 m/year. It starts with Deeba fish farm intake which established in 2018 to treat the erosion in this area. After two years of establishment of this intake, the shoreline accreted nearly 110 meters. This accretion provided land which used to construct the polyproline factory. The accretion zone extends to Zohr gas field, that has two jetties established in 2016 protected the area from erosion and turned it to accretion. Subzone B is the area in front of the Zohr gas field, which has very high accretion LRR rates with a mean value of +1.901 m/year. Subzone C is the area in front of the system of groins west of EL-Gamil first intake of el Manzala lake. this system of groins established in 2016 to trap longshore sediment to protect the intake from sedimentation. It has very high LRR accretion mean rate equals value of +7.00 m/year. Zone four starts from the system of groins upstream of the first inlet of EL-Gamil to the end of the seawall that is downstream of the second EL-Gamil inlet. It can be divided into three subzones (A, B, and C). the subdivision depends on the changes in LRR rates pattern and the behavior of each zone. First subzone A, consists of 50 transects with a total length of 2500. It has LRR mean accretion rate value of +4.85 m/year, and it is classified as a very high accretion. The main reason for these high rates of accretion is the system of groins at the start of the subzone upstream of the first inlet and the accretion and stability of shoreline in the downstream till 2015, then it turned into erosion from 2015 to 2020 due to establishment of many coastal structures in the last decade which led to prevent large amount of longshore sediment to reach this zone

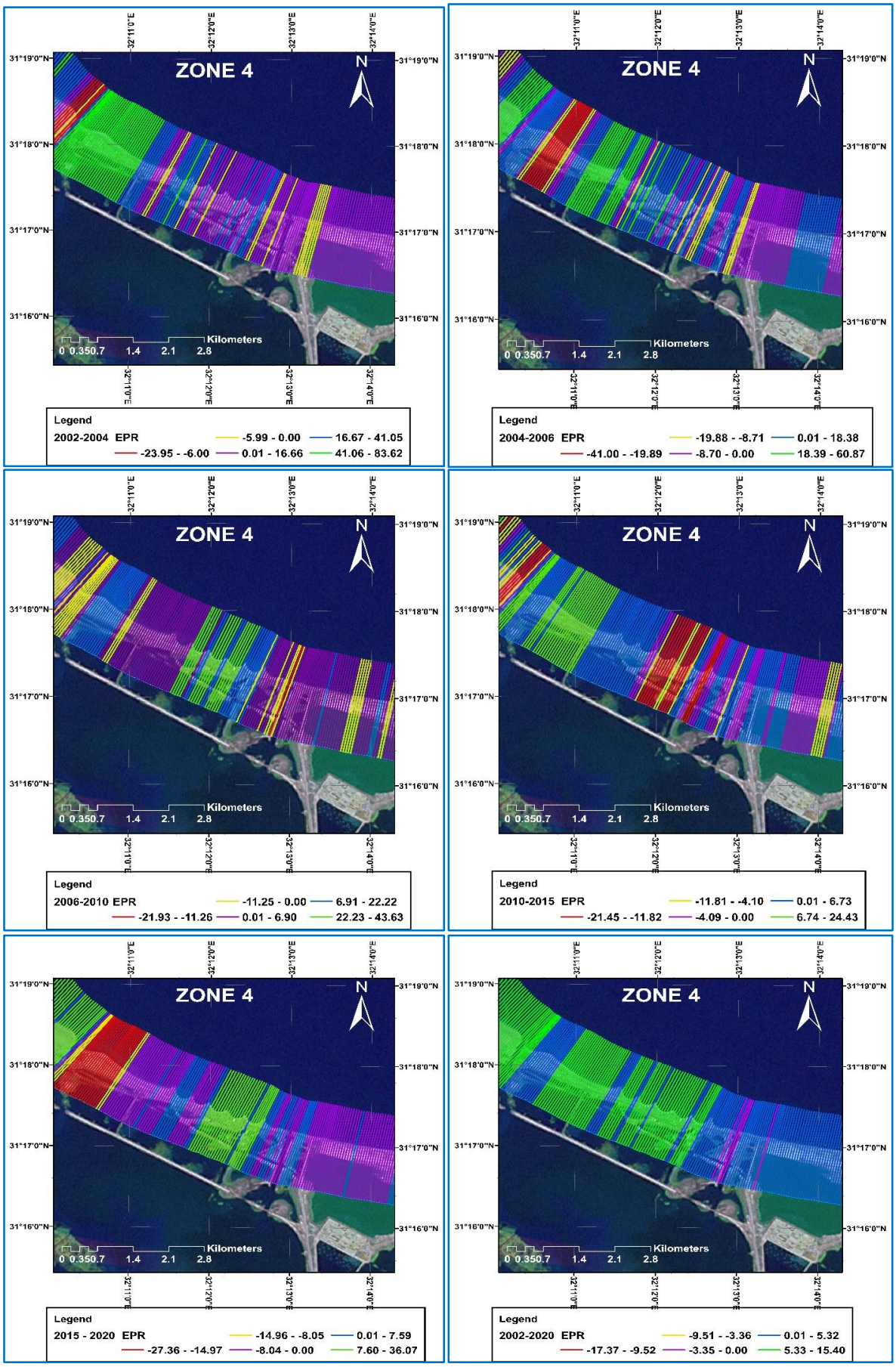

Fig. 8. Qualitative analysis for determining erosion/accretion transects using EPR which functionalized in DSAS in the five successive periods based on the digitized shorelines in 2002, 2004, 2006, 2010, 2015, and 2020.

TABLE III
SUMMARY OF EPR AND NSM MAXIMUM EROSION / ACCRETION RATES FOR THE FIVE SUCCESSIVE ZONES DURING THE PERIOD FROM 2002 TO 2020.

Periods			2002-2004	2004-2006	2006-2010	2010-2015	2015-2020	2002-2020
Zone 1	*Total number of transects*		147	147	147	147	147	147
	Baseline length		36869	36869	36869	36869	36869	36869
	NSM	NSM mean accretion	7.54	8.49	10.11	4.41	6.27	0
		NSM mean erosion	-13.46	-24.688	-23.50	-35.35	-24.77	-96.40
		NSM max. accretion	46.46	24.2	36.112	5.17	26.52	0
		NSM max. erosion	-40.67	-68.30	-80.68	-106.92	-62.98	-191.07
	EPR	EPR mean accretion	3.76	4.42	2.35	0.88	1.26	0
		EPR mean erosion	-6.73	-12.34	-5.93	-7.07	-4.95	-5.355
		EPR max. accretion	23.23	12.10	9.03	1.03	5.30	0
		EPR max. erosion	-20.34	-34.15	-20.17	-21.38	-12.60	-10.61
Zone 2	*Total number of transects*		147	147	147	147	147	147
	Baseline length		36869	36869	36869	36869	36869	36869
	NSM	NSM mean accretion	18.22	8.49	26.6	22.05	8.90	23.76
		NSM mean erosion	-10.20	-27.82	-34.73	-56.90	-53.60	-147.781
		NSM max. accretion	36.20	21.57	43.30	58.62	15.93	38.75
		NSM max. erosion	-37.86	-82.0	-87.71	-107.27	-114.48	-312.62
	EPR	EPR mean accretion	9.60	4.25	6.65	11.72	1.78	1.32
		EPR mean erosion	-5.27	-13.91	-8.86	-11.38	-10.72	-8.20
		EPR max. accretion	18.03	10.79	10.82	11.72	3.19	2.15
		EPR max. erosion	-18.93	-41.0	-21.93	-21.45	-22.90	-17.37
Zone 3	Total number of transects		147	147	147	147	147	147
	Baseline length		36869	36869	36869	36869	36869	36869
	NSM	NSM mean accretion	24.34	18.2	32.15	23.79	62.04	103.17
		NSM mean erosion	-12.67	-21.5	-18.08	-27.55	-46.62	-99.99
		NSM max. accretion	90.8	81.9	67.06	122.16	180.33	277.13
		NSM max. erosion	-29.44	-37.94	-33.53	-67.23	-114.40	-165.95
	EPR	EPR mean accretion	12.55	9.09	8.04	4.75	12.40	5.732
		EPR mean erosion	-6.33	-10.76	-4.52	-5.51	-9.32	-5.55
		EPR max. accretion	45.40	40.59	16.67	24.43	36.07	15.40
		EPR max. erosion	-14.72	-18.97	-8.38	-13.45	-22.88	-9.22
Zone 4	*Total number of transects*		147	147	147	147	147	147
	Baseline length		36869	36869	36869	36869	36869	36869
	NSM	NSM mean accretion	50.11	29.97	38.43	22.36	38.59	81.37
		NSM mean erosion	-12.77	-17.77	-9.0	-30.00	-32.61	-6.068
		NSM max. accretion	167.24	121.74	174.5	71.23	128.68	214.01
		NSM max. erosion	-47.9	-58.84	-53.96	-81.14	-136.78	-23.25
	EPR	EPR mean accretion	25.67	15.16	9.60	4.47	7.57	4.52
		EPR mean erosion	-6.39	-9.05	-2.25	-6.00	-6.59	-0.336
		EPR max. accretion	83.62	60.78	43.63	14.25	25.74	11.89
		EPR max. erosion	-23.59	-29.42	-13.49	-16.23	-27.60	-1.29
ZONE 5	*Total number of transects*		150	150	150	150	150	147
	Baseline length		36869	36869	36869	36869	36869	36869
	NSM	NSM mean accretion	17.735	8.16	15.26	24.19	3.87	31.29
		NSM mean erosion	0	-8.17	-11.91	-7.97	-19.41	-2.068
		NSM max. accretion	35.20	28.56	60.18	65.10	11.98	68.95
		NSM max. erosion	0	-22.69	-29.57	-34.64	-52.14	-3.59
	EPR	EPR mean accretion	8.867	4.08	3.81	4.83	0.774	1.738
		EPR mean erosion	0	-4.07	-3.79	-1.59	-3.88	-0.116
		EPR max. accretion	17.60	14.28	15.04	13.02	2.40	3.83
		EPR max. erosion	0	-11.35	-7.40	-1.97	-10.43	-0.20

Second subzone B, classified as accretion zone with LRR rates varying from +13.42 west of the sell to zero at the eastern end of the zone. It has LRR mean value of +6.10 m/y, which is classified as very high accretion. The main reason for these high rates of accretion is the three detached breakwaters and the western jetty of the second inlet. subzone C starts from downstream of the jetty of the second inlet along the seawall to the end of zone 4. It has negligible LRR rates that vary from -1.11 m/y to +1.14 m/y with a mean value of +0.26 m/year. Zone 5 stats from the end of the seawall that is located downstream EL-Gamil second inlet to the upstream of the Suez Canal western jetty. it can be divided into three subzones (A, B, and C). the control point of this subdivision is the behavior of the shoreline change rates. In zone A which starts from transect 589 to transect 638, the rates differ between erosion and accretion with small values ranges from + 1.18 m/year to -0.54m/year with mean value +0.25 m/year.

This value is classified as moderate accretion which don't need any protection works. For zone B that located between transect 639 to 688, the LRR rates pattern started to increase gradually from values almost near zero to the peak LRR accretion value + 3.78 m/year. The mean value of zone B is + 1.74 m/year. Zone C is located between transect 689 to 738. The rates of accretion have mean value of +3.20 m/year which classified as high accretion. These high rates of accretion along the coastline of zone 5 result from the protection structures. One of them is the system of groins that consists of 14 groins with separation distance 175 m. This system of groins led to gain land area which can be used for tourist and recreational purposes. This example achieves the meaning of sustainable development of coastal areas.

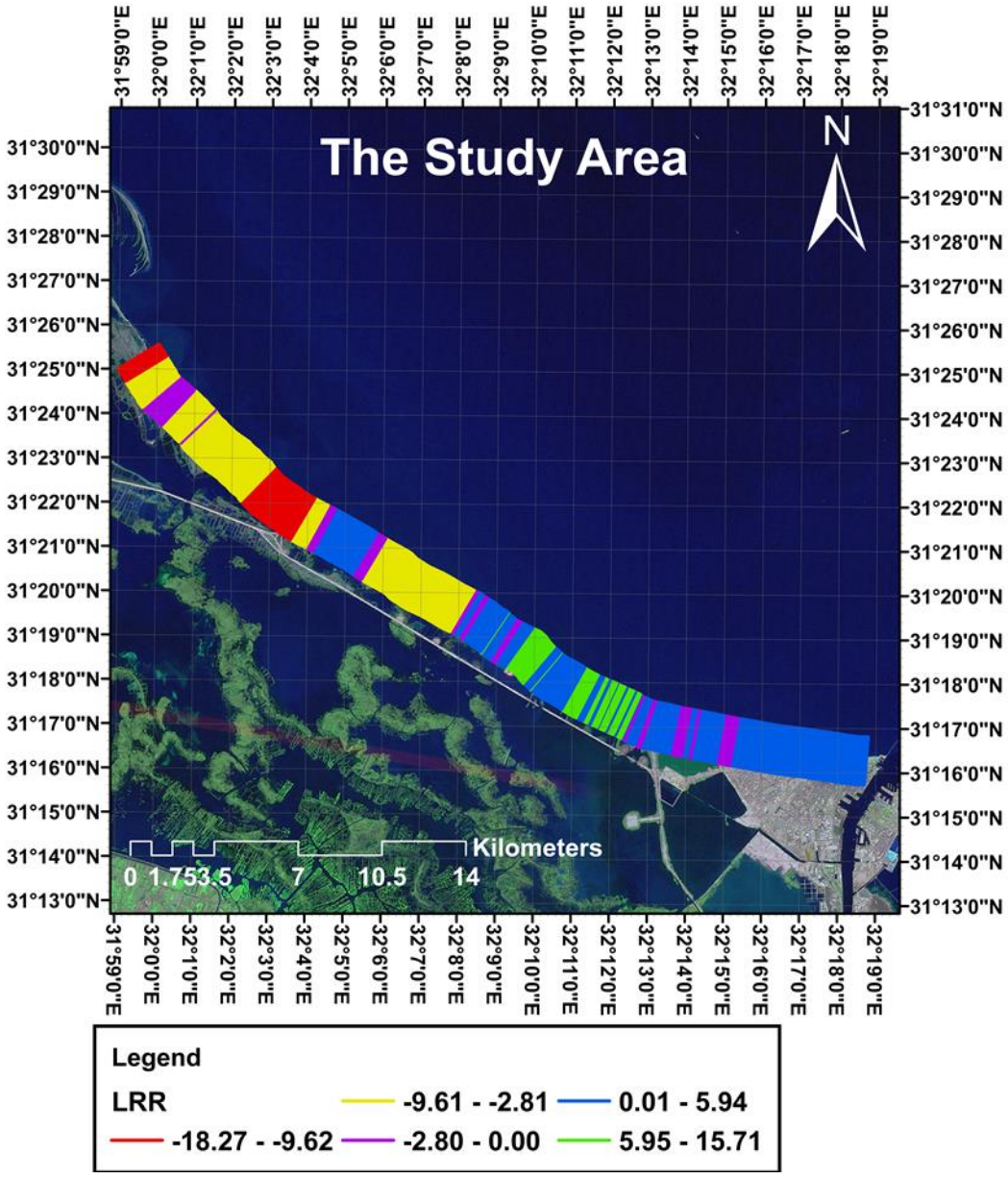

Fig. 9. Qualitative analysis for determining erosion/accretion transects using LRR which functionalized in DSAS based on the digitized shorelines in 2002, 2004, 2006, 2010, 2015, and 2020

TABLE IV
SHORELINE EVALUATION BY DECISION MATRIX AND RISK EVALUATION FOR THE STUDY AREA BY LRR FOR THE FIVE SUCCESSIVE PERIODS

Zone 1 location LRR rates (m/year)	Sector	Length	Transect id &No. of transects	LRR mean m/year	Evaluation	Risk level	Decision
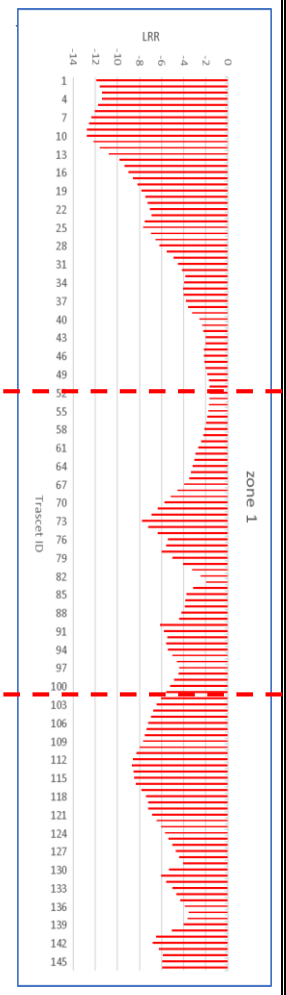	A	2500	1 50 **50**	-6.52	Very High erosion		Need different type of protection
	B	2500	51 100 **50**	-3.93	Very High erosion		Need different type of protection
	C	2250	101 147 **47**	-5.96	Very High erosion		Need different type of protection
Zone 2 location LRR rates (m/year)	**Sector**	**Length**	**Transect id & No. of transects**	**LRR mean m/year**	**Evaluation**	**Risk level**	**Decision**
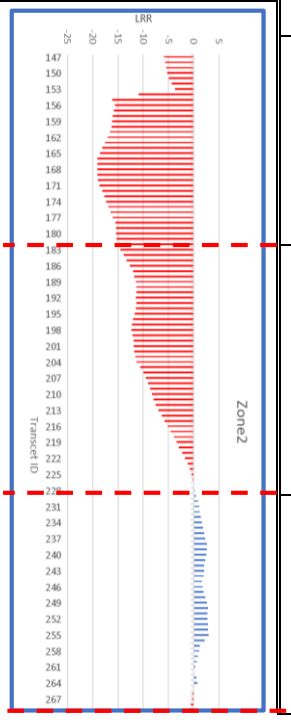	A	1650	148 181 34	-14.13	Very High erosion		Sand by pass or sand nourishment
	B	2250	182 227 46	--8.98	Very High erosion		sand nourishment or artificial protection
	C	1850	228 266 39	+1.52	High accretion		No need to any artificial protection

continued on the next page

TABLE IV: continued

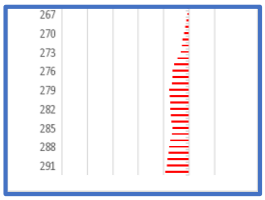

D	**1300**	**267 294 28**	**-3.20**	**Very High erosion**		sand nourishment or artificial protection

Zone 3 location LRR rates (m/year)

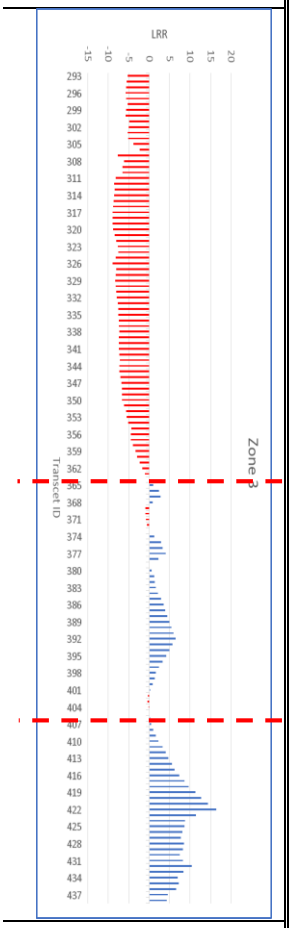

Sector	Length	Transect id &No. of transects	LRR mean (m/year)	Evaluation	Risk level	Decision
A	3650	295 367 73	-5.88	Very High erosion		Sand by pass or sand nourishment
B	2000	368 407 40	+1.901	Very High accretion		No need to any artificial protection
C	1700	408 441 34	+7.00	Very High accretion		No need to any artificial protection

Zone 4 location LRR rates (m/year)

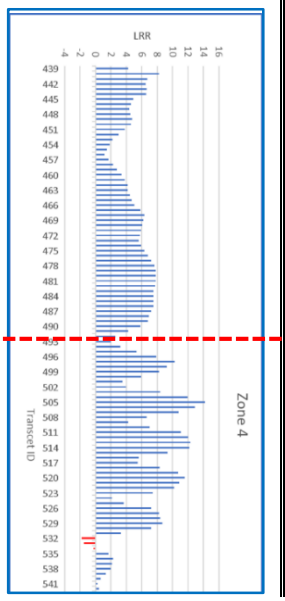

Sector	Length	Transect id &No. of transects	LRR mean (m/year)	Evaluation	Risk level	Decision
A	2500	442 491 50	+4.85	Very High accretion		No need to any artificial protection
B	2500	492 541 50	+6.10	Very High accretion		No need to any artificial protection

continued on the next page

TABLE IV: continued

Zone 5 location LRR rates (m/year)	Sector	Length	Transect id &No. of transects	LRR mean (m/year)	Evaluation	Risk level	Decision
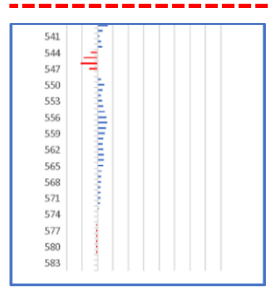	C	2250	542 588 47	+0.26	Moderate accretion		No need to any artificial protection
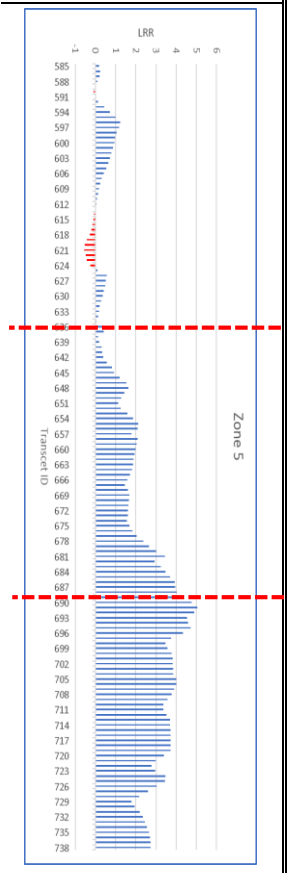	A	2500	589 638 50	+0.25	Moderate accretion		No need to any artificial protection
	B	2500	639 688 50	+1.74	High accretion		No need to any artificial protection
	C	2500	689 738 50	+3.20	Very High accretion		No need to any artificial protection

V. CONCLUSIONS AND RECOMMENDATIONS

The shoreline from Damietta to Port Said is considered one of the most valuable shorelines in Egypt. The main reason for the importance of this shoreline is the presence of many important investments located along this area, such as petrochemicals industry, fish farms and water intakes for EL-Manzala lake. Long-term shoreline changes were studied using high-accuracy remote sensing and GIS technologies. a Quantitative Study was conducted using multi-temporal satellite images over 18 years from 2002 to 2020 using automated DSAS calculations. Six shorelines were extracted with a histogram threshold of band 5 using ARCGIS 10.5 in 2002, 2004, 2006, 2010, 2015, and 2020. The results show that the maximum LRR erosion/accretion rates for the five zones were -12.19, -18.27, -8.75, -1.60, and-0.54 m/year for erosion, and zero, +2.73, +15.71, +13.42 and +4.71 m/year for accretion within the successive periods, respectively. In general, the western spit prevents the sediment transport to the study area so the western part of the area suffers from high erosion which decreases gradually toward the middle part of the study area. The eroded sediment from the first 20 km of the area deposit within the eastern part of the area toward Suez Canal jetty. On the other hand, the exist of different types of coastal protections within the study area (groins, jetties, detached breakwater…. etc.) affect the shoreline locally around the structure according to the structure type and dimensions. To control the shoreline problems, it is recommended to use sand nourishment west of the study are to control the very high erosion rate as well as sand bypass around the coastal structures to allow longshore sediment transport.

AUTHORS CONTRIBUTION

Conception or design of work: *Prof. Dr. Moheb Mina Iskander/ Eng. Ahmed Tharwat Sarhan.*

Data Collection and tools: *Eng. Ahmed Tharwat Sarhan*

Data analysis and interpretation*: Eng. Ahmed Tharwat Sarhan*

Funding acquisition: There is no funding for the research

Investigation: *Eng. Ahmed Tharwat Sarhan / Dr. Karim Nassar*

Methodology: *Prof. Dr. Moheb Mina Iskander / Eng. Ahmed Tharwat Sarhan*

Project administration: *Prof. Dr. Mahmoud El Gamal/ Prof. Dr. Moheb Mina Iskander*

Resources: *Prof. Dr. Mahmoud El Gamal/ Prof. Dr. Moheb Mina Iskander / Dr. Karim Nassar / Eng. Ahmed Tharwat Sarhan*

Software: Eng. *Ahmed Tharwat Sarhan /Prof. Dr. Moheb Mina Iskander / Dr. Karim Nassar*

Supervision: *Prof. Dr. Mahmoud El Gamal/ Prof. Dr. Moheb Mina Iskander / Dr. Karim Nassar*

Drafting the article: *Eng. Ahmed Tharwat Sarhan*

Critical revision of the article: *Prof. Dr. Moheb Mina Iskander*

FUNDING STATEMENT:

No financial support was received

DECLARATION OF CONFLICTING INTERESTS STATEMENT: The author declared that there are no potential conflicts of interest with respect to the research authorship or publication of this article.

REFERENCES

[1] A. A. Alesheikh, A. Ghorbanali, and N. Nouri, "Coastline change detection using remote sensing," *Int. J. Environ. Sci. Technol.*, vol. 4, no. 1, pp. 61–66, 2007, doi: 10.1007/BF03325962.

[2] D. J. Stanley and A. G. Warne, "Nile delta: Recent geological evolution and human impact," *Science (80-.).*, vol. 260, no. 5108, pp. 628–634, 1993, doi: 10.1126/science.260.5108.628.

[3] K. Dewidar and O. Frihy, "Pre- and post-beach response to engineering hard structures using Landsat time-series at the northwestern part of the Nile delta, Egypt," *J. Coast. Conserv.*, vol. 11, no. 2, pp. 133–142, 2007, doi: 10.1007/s11852-008-0013-z.

[4] M. M. E. Banna and M. E. Hereher, "Detecting temporal shoreline changes and erosion/accretion rates, using remote sensing, and their associated sediment characteristics along the coast of North Sinai, Egypt," *Environ. Geol.*, vol. 58, no. 7, pp. 1419–1427, 2009, doi: 10.1007/s00254-008-1644-y.

[5] K. Nassar, W. E. Mahmod, H. Fath, A. Masria, K. Nadaoka, and A. Negm, "Shoreline change detection using DSAS technique: Case of North Sinai coast, Egypt," *Mar. Georesources Geotechnol.*, vol. 37, no. 1, pp. 81–95, 2019, doi: 10.1080/1064119X.2018.1448912.

[6] M. A. Islam, M. S. Hossain, T. Hasan, and S. Murshed, "Shoreline changes along the Kutubdia Island, south east Bangladesh using digital shoreline analysis system," *Bangladesh J. Sci. Res.*, vol. 27, no. 1, pp. 99–108, 2016, doi: 10.3329/bjsr.v27i1.26228.

[7] T. Sarhan, N. Mansour, and K. Nassar, "El-Hammra Port At Northwestern Coast of Egypt of El-Hammra Port At Northwestern Coast of Egypt," no. May, 2020.

[8] M. M. Iskander, "Wave Climate and Coastal Structures in the Nile Delta Coast of Egypt," *Emirates J. Eng. Res.*, vol. 18, no. 1, pp. 43–57, 2013.

[9] A. M. Khalifa, M. R. Soliman, and A. A. Yassin, "Assessment of a combination between hard structures and sand nourishment eastern of Damietta harbor using numerical modeling," *Alexandria Eng. J.*, vol. 56, no. 4, pp. 545–555, 2017, doi: 10.1016/j.aej.2017.04.009.

[10] I. Sekovski, F. Stecchi, F. Mancini, and L. Del Rio, "Image classification methods applied to shoreline extraction on very high-resolution multispectral imagery," *Int. J. Remote Sens.*, vol. 35, no. 10, pp. 3556–3578, 2014, doi: 10.1080/01431161.2014.907939.

[11] U. Natesan, A. Parthasarathy, R. Vishnunath, G. E. J. Kumar, and V. A. Ferrer, "Monitoring Longterm Shoreline Changes along Tamil Nadu, India Using Geospatial Techniques," *Aquat. Procedia*, vol. 4, no. July, pp. 325–332, 2015, doi: 10.1016/j.aqpro.2015.02.044.

Arabic Title:

تتبع تغير خط الشاطئ باستخدام نظام التحليل الرقمي لخط الشاطئ: منطقة الدراسة خط الشاطئ بين دمياط وبورسعيد

Arabic Abstract:

تعاني دلتا النيل في مصر من العديد من المشاكل الساحلية بسبب العوامل الطبيعية والبشرية خاصة الجزء الشرقي من دمياط إلى بورسعيد. تهدف هذه الورقة البحثية إلى دراسة المشاكل الساحلية في هذا الجزءمن دلتا النيل. يعتمد هذا الاستقصاء على رصد وتيرة تغير الخط الساحلي على طول ساحل دمياط بورسعيد. استخدم نظام تحليل الخط الساحلي الرقمي لتحليل معدلات تغير الخط الساحلي DSASو الذي هو إمتداد لبرنامج ARCGIS 10.5 .

استخدمت ست صور أقمار صناعية لسنوات مختلفة كالآتي: (2002، 2004، 2006، 2010، 2015 و2020) للكشف عن تآكل السواحل وأنماط التراكم لمنطقة الدراسة. تم تصحيح هذه الصور هندسيًا لاستخدامها في تحليل معدلات تغير الخط الساحلي. تم استخدام أداة تغير خط الشاطئ باستخدام ثلاث طرق وهي: معدل نقطة النهاية (EPR) و معدل الانحدار الخطي (LRR) وصافي حركة الخط الساحلي (NSM).

أظهرت النتائج أن منطقة الدراسة واجهت العديد من التغيرات الساحلية التي تختلف بين الترسيب والنحر. من الواضح أن الهياكل الساحلية والأنشطة البشرية والقوى الهيدروديناميكية هي الأسباب الرئيسية لتغيرات السواحل داخل منطقة الدراسة